J Pharmacol Sci **108**, 320 – 334 (2008)

Journal of Pharmacological Sciences

Full Paper

Gene Expression Profiling Reveals Complex Changes in the Olfactory Bulbectomy Model of Depression After Chronic Treatment With Antidepressants

Kou Takahashi[1], Akiyoshi Saitoh[2], Misa Yamada[1], Yoshiaki Maruyama[1], Noritaka Hirose[2], Junzo Kamei[2], and Mitsuhiko Yamada[1,*]

[1]*Department of Psychogeriatrics, National Institute of Mental Health, National Center of Neurology and Psychiatry, 4-1-1 Ogawahigashimachi, Kodaira, Tokyo 187-8553, Japan*
[2]*Department of Pathophysiology and Therapeutics, School of Pharmacy and Pharmaceutical Sciences, Hoshi University, Tokyo 142-8501, Japan*

Received June 13, 2008; Accepted September 24, 2008

Abstract. We investigated the effects of antidepressants on the gene expression profile and behavior of olfactory-bulbectomized (OBX) rats. Removal of the main olfactory bulbs in rats alters neuronal function in brain areas involved in emotional regulation, resulting in maladaptive behavioral patterns similar to the symptoms of patients with depression. Previously, we found that OBX-induced behavioral and neuronal abnormalities were completely rescued by chronic treatment with SNC80, an opioid delta agonist, as well as with classical monoaminergic antidepressants. Thus, to determine the basis for this effect, we analyzed gene expression in OBX rat frontal cortex using a GeneChip® rat Genome oligonucleotide array after imipramine or SNC80 treatment. We found that imipramine and SNC80 induced the following systematic changes in OBX rats: zinc ion binding; hydrolase activity, acting on acid anhydrides, in phosphorus-containing anhydrides; protein serine/threonine kinase activity; N-acetyltransferase activity; protein modification process; regulation of cellular process; and regulation of neurotransmitter levels. Defining the roles of candidate neuronal systems in antidepressant-induced neural changes are likely to transform the course of research on the biological basis of mood disorders.

Keywords: antidepressant, delta opioid receptor, olfactory bulbectomy, gene expression, model animal

Introduction

Antidepressants are very effective agents for preventing and treating depression and have been used clinically for more than 50 years. Typical antidepressants significantly increase the synaptic concentration of norepinephrine and/or serotonin. However, a latency period of several weeks generally elapses before therapeutic effects of antidepressants are observed. This delayed action could be due to either the indirect regulation of other neuronal signal transduction systems or the regulation of gene transcription following chronic treatment. Indeed, antidepressants have been shown to affect the expression of immediate early genes and transcription factors, including c-fos, FosB, junB, NGF1-A, and CREB (1). These regulatory proteins activate or repress genes that encode specific proteins and may be involved in antidepressant-induced alterations of central nervous system (CNS) function.

Pharmacogenomics is a powerful tool that can be used to identify neuronal systems affected by antidepressants. GeneChip® technology, which is one of the most useful tools of pharmacogenomics, can determine the expression of several tens of thousands of genes and can help us understand the state of the brain after chronic antidepressant treatments. GeneChip® analysis has been

*Corresponding author. mitsu@ncnp.go.jp
Published online in J-STAGE
doi: 10.1254/jphs.08149FP

used to study the effects of chronic antidepressant treatment in normal animals (2, 3), and some candidate genes and hypotheses about antidepressant actions have been indicated. However, the effect of antidepressants on gene expression in animal depression models is not well understood. Hence, comprehensive gene expression analysis in a valid animal model of depression in which antidepressants are applied is much needed.

The olfactory bulbectomized (OBX) rat is considered to be one of the important animal models of depression in terms of face and predictive validity. Olfactory bulbectomy results in a complex constellation of behavioral, neurochemical, neuroendocrine, and neuroimmune alterations, many of which reflect symptoms reported in patients with major depression (4). These changes typically require 1 – 2 weeks to develop, and they occur independent of sensory deprivation (4, 5). Many investigators have demonstrated that the behavioral effects of olfactory bulbectomy include an abnormal, stress-induced increase in locomotor activity and increases in various measures of irritability and hyperemotionality (6 – 11). Such behaviors resemble psychomotor agitation, a diagnostic criterion for depression. In addition, olfactory bulbectomy has been reported to alter adrenergic, serotonergic, and excitatory amino acid receptors in cortical and limbic areas in a fashion similar to the receptor alterations observed in suicide victims, and immune functions are suppressed in a manner consistent with the immunosuppression seen in clinical depression (5, 7, 9, 12). Other models of depression such as learned helplessness and chronic mild stress (13, 14) react to acute antidepressant treatment. By contrast, OBX rats are unique in their sensitivity to chronic but not acute administration of clinically efficacious antidepressants (15 – 20).

We have recently reported that the nonpeptidic delta-opioid agonist SNC80 displays naltrindole-sensitive antidepressant-like properties in OBX rats (21). The delta-opioid receptor system is sometimes associated with symptoms of depression as well as with antidepressant effects. Delta-opioid receptor knockout mice exhibit depressive-like responses in the forced swim test and anxiogenic-like responses in the elevated plus-maze test (22). In addition, activation of the delta-opioid receptor has antidepressant-like properties in many animal models. BUBU, a selective delta-opioid agonist, showed antidepressant-like effects in the learned helplessness model of depression (23). Increasing levels of endogenous delta-opioid peptides with enkephalinase inhibitors such as RB101 result in antidepressant-like effects in the forced swim test and the learned helplessness model of depression (23, 24).

In the present study, we used GeneChip® technology to carry out the first ever comprehensive gene expression analysis of OBX rats treated with imipramine and SNC80, two drugs with different mechanisms of action. We sought to identify the functional class of genes affected by drug treatments and aimed to advance our hypothesis on the mechanism underlying antidepressant action. It is reasonable to assume that interactions exist among neuronal systems involved in the mechanism of antidepressant action; we tried to identify neuronal systems in OBX rats affected by imipramine and/or SNC80.

Materials and Methods

Drugs

The drugs used in the present study were imipramine (Sigma Chemical Co., St. Louis, MO, USA) and (+)-4-[(alpha*R*)-alpha-((2*S*,5*R*)-4-allyl-2,5-dimethyl-1-piperazinyl)-3-methoxybenzyl]-*N*,*N*-diethylbenzamide (SNC80) (Toray Industries, Inc., Tokyo). All drugs were dissolved in physiological saline. Rats were injected s.c. at a drug dose of 1.0 ml/kg body weight.

Animals

Sixteen male 8-week-old (200 – 240 g) Wistar rats (Tokyo Laboratory Animals Science, Tokyo) were used. They had free access to food and water in an animal room that was maintained at 22 ± 1°C with a 12-h light-dark cycle (lights on automatically at 8:00 a.m.). This study was carried out in accordance with the Guide for the Care and Use of Laboratory Animals of Hoshi University, which is accredited by the Japanese Ministry of Education, Culture, Sport, Science, and Technology.

Olfactory bulbectomy–induced hyperemotionality in rats

Animals were anesthetized with sodium pentobarbital (40 mg/kg, i.p.) and placed in a stereotactic apparatus (ASI Instruments, Inc., Warren, MI, USA). The olfactory bulbs were removed by suction. Postoperatively, animals were housed in single cages. At 14 days post-surgery, hyperemotionality was measured using a modified procedure (25, 26). Rats' responses were scored to the following stimuli: i) The "attack response" was scored by presenting a rod 4 – 5 cm in front of the rat's snout; ii) the "startle response" was scored by blowing air onto the rat's dorsum (air was delivered through a 5-ml syringe); iii) the "struggle response" was scored by handling the rat with a gloved hand; and iv) the "fight response" was scored by pinching the rat's tail with a mosquito forceps. A trained researcher performed these operations. The responses were graded as follows: 0, no response; 1, slight response; 2, moderate

response; 3, marked response; and 4, extreme response. For each emotional response, vocalization during the test was also scored and graded as follows: 0, no vocalization; 1, occasional vocalization; and 2, marked vocalization. The vocal score was added to each emotional response score.

We measured the emotional response score of each animal within 5 min in one day. Only rats that exhibited hyperemotionality (score: >14) were selected for further study in the drug administration experiments. Imipramine (10 mg/kg) or SNC80 (10 mg/kg) was administered once daily for a total of 7 days. On the 8th day after the 14-day post-surgical period, emotional responses were measured 24 h after drug administration. The observers were kept unaware of the drug treatment. We determined the effective dose of imipramine and SNC80 according to our previous experiments (21, 27)

Data are expressed as means ± S.E.M. Statistically significant differences between groups were assessed with one-way analysis of variance (ANOVA) followed by the Tukey-Kramer test. Analyses were made using StatView statistical software SAS system Ver. 6.12 (SAS Institute, Inc., Cary, NC, USA).

Sample preparation for GeneChip®

After the emotional response measurements, total RNA was extracted from rat frontal cortex using the Isogen reagent (Nippon Gene Co., Tokyo). Micorarray analysis was performed according to the manufacturer's protocol (Affymetrix, Santa Clara, CA, USA). Briefly, 5 μg of total RNA was used for cDNA synthesis by oligo-dT and SuperScript II reverse transcriptase, followed by in vitro transcription and biotin labeling. Biotinylated cRNA was fragmented, and 15 μg of the fragmented cRNA was hybridized to a GeneChip® Rat Genome 230 2.0 array (Affymetrix), which contains probes for about 30,000 genes. The quality of total RNA and cRNA was analyzed on a BioAnalyzer (Agilent Technologies, Inc., Santa Clara, CA, USA). Each sample from an individual rat was hybridized to an array. The samples were hybridized at 45°C for 16 h under constant rotation (60 rpm) using a GeneChip® Hybridization Oven 640 (Affymetrix). After hybridization, microarrays were washed, stained with streptavidin phycoerythrin in a GeneChip® Fluidics Station 450 (Affymetrix), and scanned in a GeneChip® Scanner 3000 (Affymetrix).

Quality control criteria

Tissue preparations and RNA extractions were performed on a single batch by the same investigator in order to minimize experimental variability. All samples yielded equal amounts of biotinylated RNA. An average of 91.8 ± 13.3 μg (mean ± S.D.) of biotinylated RNA was obtained from the frontal cortex for in vitro transcription. All quality control criteria defined by Affymetrix were met by the samples, and no differences between the experimental groups were observed. The average percent "present" call across all arrays was 66.0 ± 2.4%, and 3′/5' glyceraldehyde 3-phosphate dehydrogenase (GAPDH) was 1.3 ± 0.1 (averages ± S.D.). Background and noise were 65.6 ± 11.1 and 3.8 ± 1.3, respectively (average ± S.D.).

Data analyses

The raw microarray data were processed with Affymetrix MicroArray Suite software, version 5.0 (28). To normalize the probe intensity across different chips, the top 2% and bottom 2% of signal intensities were excluded, and then the means were calculated. The data were then imported into GeneSpring 7.2 software (Silicon-Genetics, Redwood, CA, USA). Genes that were "present" calls across all arrays were used in the hierarchical clustering analysis. Finally, 16,342 genes were analyzed. Each sample was categorized according to gene expression pattern. The functional clustering analysis and the gene expression pattern analysis used genes that were filtered by two processes: i) all "present" called genes in OBX group; ii) the difference in OBX group was within 0.5 SD. A total of 18,509 genes passed these filtering procedures. Differentially expressed genes compared with the OBX group were defined according to the following criteria: i) 1.2-fold change in each imipramine and SNC80 treatments group; ii) $P<0.05$ in the two-tailed Student's t-test in each imipramine and SNC80 treatments group. The common genes of passed criteria between imipramine and SNC80 treatments group were analyzed. For the functional clustering analysis, the resulting 577 genes were analyzed using The Database for Annotation, Visualization, and Integrated Discovery (DAVID 2.0) (released 6/2007) based on Gene Ontology (GO) annotations. DAVID is a web-based application that allows users to access relational databases for functional annotations (http://david.abcc.ncifcrf.gov/home.jsp) (29). The Fisher's exact test was applied to evaluate the statistical significance of the association between the 577 genes and GO database ($P<0.01$). GO terms were described according to the GO database (http://www.geneontology.org/).

Results

Emotional and behavioral changes after imipramine or SNC80 treatment

In the present study, we determined emotional and

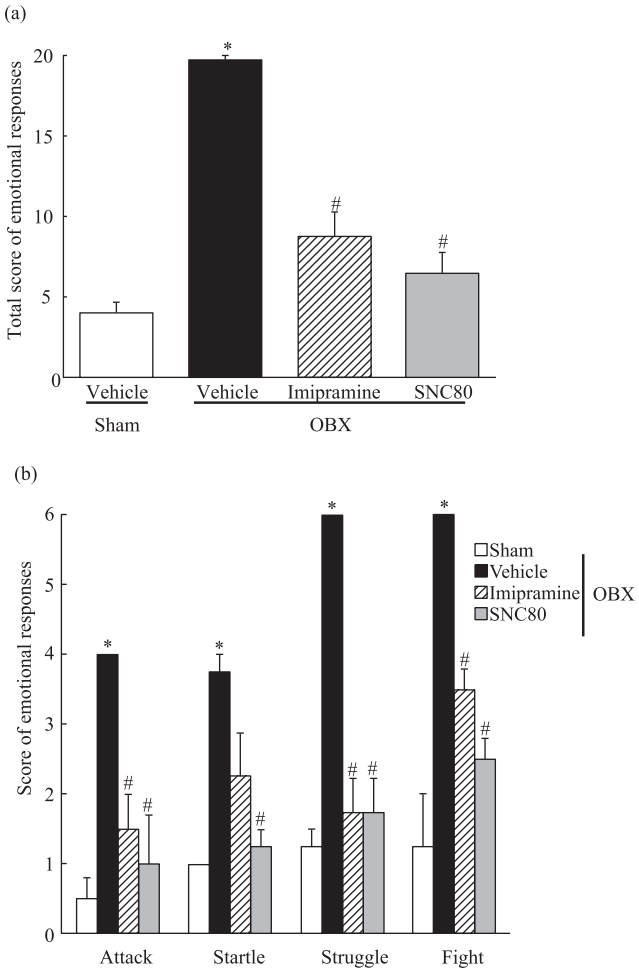

Fig. 1. Effects of chronic imipramine or SNC80 treatment on hyperemotionality of OBX rats. Drugs (10 mg/kg, s.c.) were administered once daily for 7 days. Emotional responses were measured 24 h after the last drug administration. a) Total emotional response scores and b) response scores by category. The total emotional response score represents the sum of each response score (attack, startle, struggle, and fight responses). Data are means ± S.E.M. from 4 rats. *$P<0.05$ *vs* vehicle-treated sham rats. $^{\#}P<0.05$ *vs* vehicle-treated OBX rats.

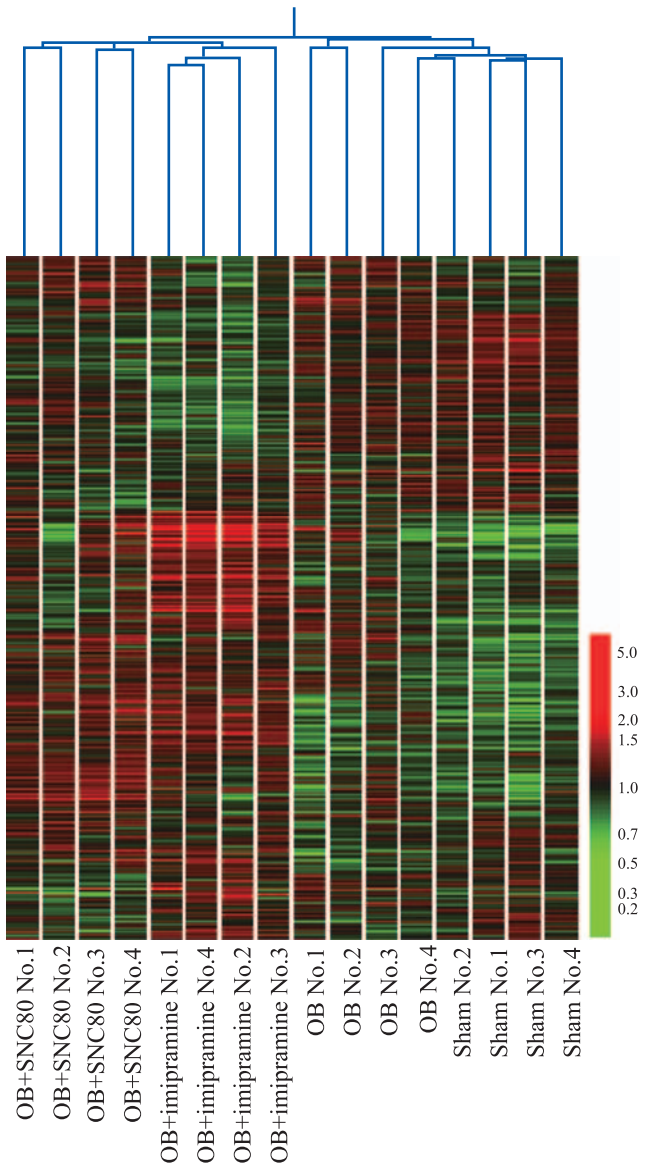

Fig. 2. Unsupervised, hierarchical clustering of all samples. We performed clustering experiments using 16,342 genes, all "present" calls across all arrays. Each column represents one sample. Upregulated genes are red and downregulated genes are green; gene expression is relative to the average gene expression across all conditions. The clustering dendrogram is displayed above the image. The organization and length of the branches in the dendrogram reflects the similarity in gene expression profiles between samples.

behavioral changes after imipramine or SNC80 treatment in OBX rats (Fig. 1). The total emotional response scores of OBX rats were significantly higher than those of sham-operated rats 14 days post-surgery. The emotional responses of OBX rats were not significantly affected by vehicle after chronic administration for 7 days (Fig. 1a). Chronic administration of imipramine or SNC80 at a dose of 10 mg/kg (i.p.), however, significantly reduced hyperemotionality in OBX rats (Fig. 1a).

The attack, startle, struggle, and fight response scores of OBX rats are shown in Fig. 1b. Vehicle-treated OBX rats clearly had significantly higher attack, startle, struggle, and fight responses than sham rats. Chronic imipramine administration (10 mg/kg, i.p.) significantly reduced the attack, fight, and struggle response scores of vehicle-treated OBX rats (Fig. 1b). Chronic SNC80 administration (10 mg/kg, i.p.) completely abolished all hyperemotionality responses in OBX rats (Fig. 1b).

Gene expression pattern after imipramine or SNC80 treatment

To address whether variations in gene expression levels can explain the effects of imipramine and SNC80

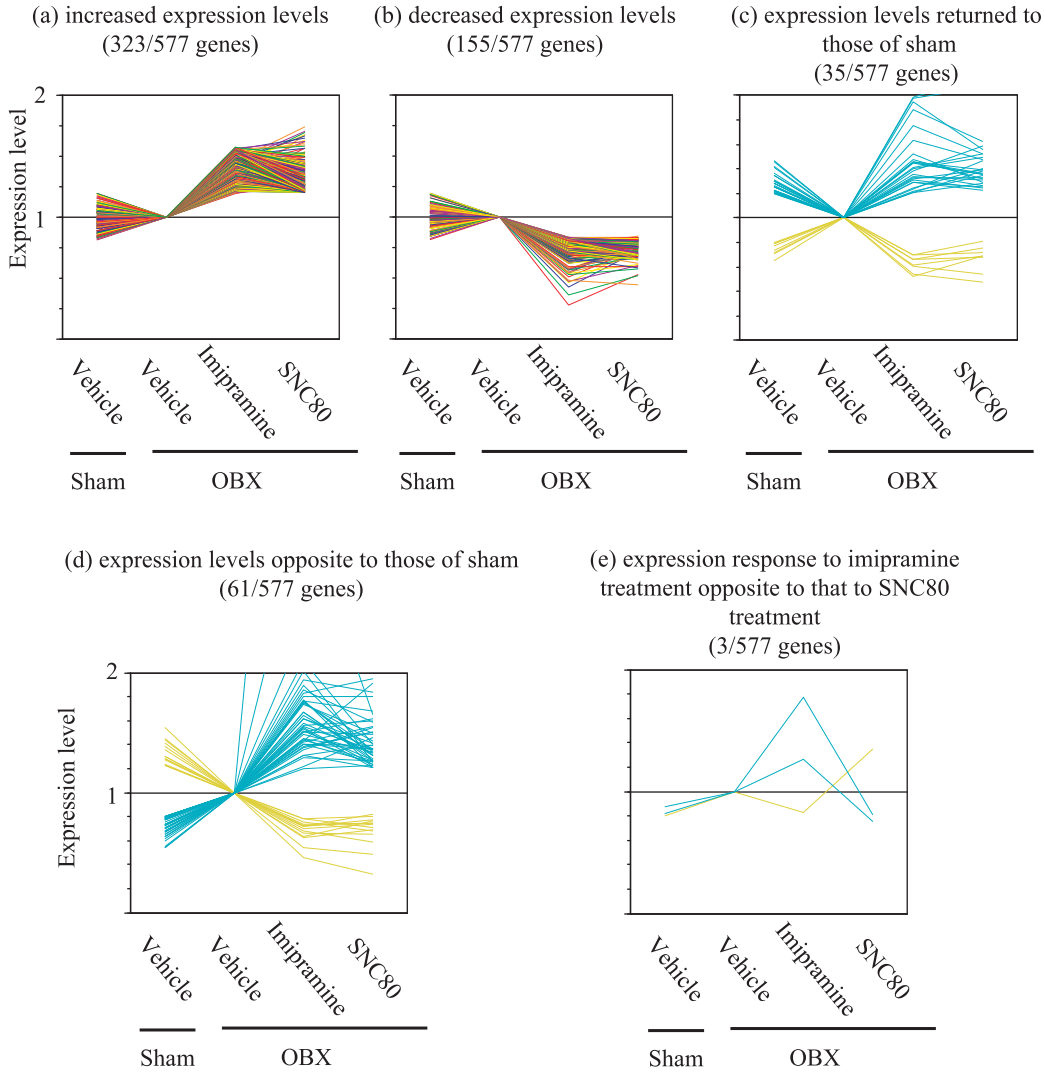

Fig. 3. Classification of imipramine- and SNC80-responding genes based on gene expression patterns. A total of 577 genes displayed significant differential expression following treatment with imipramine and SNC80. These genes were assigned to five classes based on their response to drug treatment: a: increased expression levels, b: decreased expression levels, c: expression levels returned to those of sham, d: expression levels opposite to those of sham, e: expression response to imipramine treatment opposite to that to SNC80 treatment. Up or down thresholds are set to an observed difference of 1.2-fold. The number of differentially expressed genes is listed in parentheses.

on emotional response, we performed unsupervised hierarchical clustering analysis. Samples assigned to the same cluster had similar gene expression levels, whereas samples assigned to different clusters had dissimilar gene expression levels. In this analysis, samples of the same group were assigned as a single cluster (Fig. 2).

To confirm the expression patterns, we assigned the 577 genes that showed significant differential expression to five classes (Fig. 3). Drug treatment was correlated with expression levels of 35 genes returning back to that of sham levels (Fig. 3c). Interestingly, we identified only 3 genes that responded oppositely to imipramine and SNC80 treatment (Fig. 3e).

Functional clustering after imipramine or SNC80 treatment

To determine whether the 577 genes affected by imipramine and SNC80 treatment correspond to specific functional classifications, we used supervised queries of the GO database. GO classifies genes into three main categories according to i) biological process, ii) molecular function, and iii) cellular component. Biological /functional classifications are then organized according to GO pathways, which are linked as hierarchical clusters, with the most general function positioned at a primary node and more specific functions positioned at subsequent nodes. Table 1 lists the functional classifica-

Table 1. Functional classification of genes differentially expressed in response to antidepressant treatments

Category	Term	Number of genes	*P*-value
Molecular function	Binding (GO: 0005488)	238	3.7E-09
	ion binding (GO: 0043167)	73	7.1E-05
	cation binding (GO: 0043169)	67	9.9E-06
	transition metal ion binding (GO: 0046914)	44	3.9E-05
	zinc ion binding (GO: 0008270)	38	2.7E-06
	metal ion binding (GO: 0046872)	73	7.1E-05
	transition metal ion binding (GO: 0046914)	44	3.9E-05
	zinc ion binding (GO: 0008270)	38	2.7E-06
	nucleotide binding (GO: 0000166)	54	9.3E-05
	protein binding (GO: 0005515)	129	2.7E-04
	nucleic acid binding (GO: 0003676)	70	3.2E-03
Molecular function	Catalytic activity (GO:0003824)	—	>0.01
	hydrolase activity (GO:0016787)	—	>0.01
	hydrolase activity, acting on acid anhydrides (GO: 0016817)	22	7.6E-03
	hydrolase activity, acting on acid anhydrides, in phosphorus-containing anhydrides (GO: 0016818)	22	6.8E-03
	transferase activity (GO:0016740)	—	>0.01
	transferase activity, transferring phosphorus-containing groups (GO:0016772)	—	>0.01
	kinase activity (GO: 0016301)	29	9.9E-03
	protein kinase activity (GO:0004672)	—	>0.01
	protein serine/threonine kinase activity (GO: 0004674)	19	8.9E-03
	transferase activity, transferring acyl groups (GO:0016746)	—	>0.01
	transferase activity, transferring groups other than amino-acyl groups (GO:0016747)	—	>0.01
	acyltransferase activity (GO:0008415)	—	>0.01
	acetyltransferase activity (GO:0016407)	—	>0.01
	N-acetyltransferase activity (GO:0008080)	5	5.1E-03
	N-acyltransferase activity (GO:0016410)	—	>0.01
	N-acetyltransferase activity (GO:0008080)	5	5.1E-03
Category	Term	Number of genes	*P*-value
Biological process	Metabolic process (GO: 0008152)	177	8.4E-04
	macromolecule metabolic process (GO: 0043170)	114	1.3E-04
	biopolymer metabolic process (GO: 0043283)	81	1.4E-05
	biopolymer modification (GO: 0043412)	47	1.6E-03
	protein modification process (GO: 0006464)	46	1.2E-03
	protein metabolic process (GO: 0019538)	87	2.6E-04
	cellular protein metabolic process (GO: 0044267)	80	4.5E-04
	protein modification process (GO: 0006464)	46	1.2E-03
	cellular macromolecule metabolic process (GO: 0044260)	80	7.7E-04
	cellular protein metabolic process (GO: 0044267)	80	4.5E-04
	protein modification process (GO: 0006464)	46	1.2E-03
	cellular metabolic process (GO: 0044237)	169	2.7E-04
	cellular macromolecule metabolic process (GO: 0044260)	80	7.7E-04
	cellular protein metabolic process (GO: 0044267)	80	4.5E-04
	protein modification process (GO: 0006464)	46	1.2E-03
	primary metabolic process (GO: 0044238)	161	8.1E-04
	protein metabolic process (GO: 0019538)	87	2.6E-04
	cellular protein metabolic process (GO: 0044267)	80	4.5E-04
	protein modification process (GO: 0006464)	46	1.2E-03

Biological process	Biological regulation (GO:0065007)	—	>0.01
	└regulation of biological process (GO: 0050789)	109	8.4E-06
	├regulation of cellular process (GO: 0050794)	91	6.7E-04
	└regulation of neurotransmitter levels (GO: 0001505)	9	9.0E-03
Biological process	Cellular process (GO:0009987)	—	>0.01
	└cellular component organization and biogenesis (GO: 0016043)	61	5.2E-04

Gene ontology terms are organized hierarchically, with categories of a more general nature being situated at primary, top-level branches and categories of a more specific nature situated at secondary, lower-level branches.

Table 2. Differentially expressed genes identified according to selected enriched gene ontology terms

Zinc ion binding

Symbol	Description	Accession No.	Sham		OBX + Imipramine		OBX + SNC80		Probe	
			Fold change	*P*-value	Fold change	*P*-value	Fold change	*P*-value		
Araf	V-raf murine sarcoma 3611 viral oncogene homolog	AI169278	1.06	0.212	1.23	0.001	1.26	0.019	1372550_at	
Arts1	Type 1 tumor necrosis factor receptor shedding aminopeptidase regulator	NM_030836	0.85	0.287	1.99	0.026	1.50	0.026	1368356_a_at	
Egr1	Early growth response 1	NM_012551	1.19	0.162	0.80	0.035	0.68	0.004	1368321_at	
Egr4	Early growth response 4	NM_019137	1.54	0.001	0.78	0.035	0.71	0.011	1387442_at	
Folh1	Folate hydrolase	NM_057185	0.88	0.138	1.35	0.003	1.25	0.021	1387363_at	
Gs3	Putative regulation protein GS3	NM_138856	1.19	0.107	0.62	0.012	0.70	0.028	1369543_s_at	
Ing1	Inhibitor of growth family, member 1	AI170649	0.99	0.020	0.83	0.023	0.83	0.006	1373457_at	
Lap3	Leucine aminopeptidase 3	AA945172	0.68	0.012	1.85	0.008	1.59	0.018	1376579_at	
Limd1_predicted	LIM domains containing 1 (predicted)	BI289676	0.92	0.673	1.46	0.001	1.26	0.020	1372668_at	
LOC498265	Similar to hypothetical protein FLJ10706	AI105450	0.81	0.175	1.63	0.007	1.59	0.024	1374767_at	
LOC499094	Similar to zinc finger protein 61	AI030120	0.90	0.534	1.22	0.012	1.33	0.030	1398663_at	
LOC499900	Similar to Zinc finger protein 133	AI146063	1.25	0.076	1.25	0.001	1.41	0.035	1389709_at	
LOC687633	Similar to ubiquitin protein ligase E3B	BF281133	0.95	0.195	0.71	0.002	0.81	0.000	1371728_at	
Matr3	Matrin 3	AI169689	0.89	0.540	1.45	0.007	1.49	0.022	1382522_at	
Mbd1	Methyl-CpG binding domain protein 1	BF281957	0.99	0.386	0.80	0.005	0.82	0.022	1392885_at	
Mmp14	Matrix metalloproteinase 14 (membrane-inserted)	X83537	0.55	0.051	3.32	0.006	1.65	0.011	1367860_a_at	
Myt1_predicted	Myelin transcription factor 1 (predicted)	AI070390	1.20	0.331	1.41	0.004	1.53	0.029	1392332_at	
Nqo2	NAD(P)H dehydrogenase, quinone 2	AA945624	0.86	0.573	2.29	0.000	1.87	0.011	1374959_at	
Pdcd2	Programmed cell death 2	AI704628	1.30	0.150	1.52	0.001	1.29	0.012	1371002_at	
Pias4	Protein inhibitor of activated STAT, 4	AI412927	0.96	0.467	0.71	0.007	0.81	0.015	1398352_at	
Prkch	Protein kinase C-eta	AA799981	1.18	0.126	1.47	0.002	1.62	0.004	1388836_at	
Pts	6-Pyruvoyl-tetrahydropterin synthase	NM_017220	0.93	0.171	1.55	0.030	1.45	0.038	1369304_at	
Rbx1	Ring-box 1	AI179646	0.83	0.092	1.43	0.012	1.35	0.016	1388538_at	
Rnf138	Ring finger protein 138	AW529177	1.23	0.223	1.45	0.009	1.35	0.033	1382379_at	
Rock1	Rho-associated coiled-coil forming kinase 1	NM_031098	0.96	0.729	1.76	0.017	1.52	0.002	1368932_at	
Rock2	Rho-associated coiled-coil forming kinase 2	NM_013022	0.74	0.042	0.53	0.004	0.69	0.004	1387379_at	
Tcfcp2l2	Transcription factor CP2–like 2	AI716050	0.94	0.233	1.55	0.009	1.42	0.001	1379914_at	
Trim2	Tripartite motif protein 2	H31511	1.01	0.987	1.31	0.009	1.20	0.023	1397596_at	
Trim34_predicted	Tripartite motif protein 34 (predicted)	BI280655	0.73	0.042	1.55	0.025	1.35	0.015	1385252_at	
Unc13c	Unc-13 homolog C (*C. elegans*)	U75361	0.85	0.121	0.71	0.045	0.70	0.017	1370546_at	
Usp40	Ubiquitin specific protease 40	BM391750	0.87	0.048	1.34	0.002	1.31	0.014	1390492_a_at	
Yme1l1	YME1 (*S. cerevisiae*)–like 1	AA849923	1.21	0.252	1.98	0.022	2.07	0.000	1385999_at	
Zcchc11_predicted	Zinc finger, CCHC domain containing 11 (predicted)	BE108198	0.97	0.754	1.46	0.007	1.47	0.003	1390820_at	
Zfhx1b	Zinc finger homeobox 1b	AW529031	0.84	0.487	1.36	0.016	1.26	0.014	1390940_at	
Zfhx1b	Zinc finger homeobox 1b	BG377397	0.79	0.778	1.43	0.005	1.91	0.004	1393795_at	
Zfp131	Zinc finger protein 131	AA924380	0.99	0.520	1.67	0.008	1.51	0.012	1393780_at	
Zfp347	Zinc finger protein 347	AB047638	0.94	0.519	1.66	0.047	1.26	0.027	1368726_a_at	
Zfp446_predicted	Zinc finger protein 446 (predicted)	BM389392	1.03	0.569	1.35	0.030	1.22	0.009	1391702_at	
Znf386	Zinc finger protein 386 (Kruppel-like)	NM_019620	0.82	0.066	1.43	0.014	1.25	0.044	1368712_at	

Hydrolase activity, acting on acid anhydrides, in phosphorus-containing anhydrides

Symbol	Description	Accession No.	Sham		OBX + Imipramine		OBX + SNC80		Probe	
			Fold change	*P*-value	Fold change	*P*-value	Fold change	*P*-value		
Abca8b_predicted	ATP-binding cassette, sub-family A (ABC1), member 8b (predicted)	BF386852	1.08	0.661	1.40	0.005	1.62	0.019	1395644_at	
Abcb6	ATP-binding cassette, sub-family B (MDR/TAP), member 6	NM_080582	1.09	0.459	0.65	0.005	0.78	0.024	1368159_at	
Abcc6	ATP-binding cassette, sub-family C (CFTR/MRP), member 6	NM_031013	1.01	0.778	1.41	0.046	1.35	0.011	1368452_at	
Abcg3	ATP-binding cassette, sub-family G (WHITE), member 3	BF282804	0.78	0.048	1.76	0.003	1.36	0.017	1393217_at	
Chd6_predicted	Chromodomain helicase DNA binding protein 6 (predicted)	BF398050	0.87	0.302	1.37	0.048	1.36	0.025	1379580_at	
Ddx21a	DEAD (Asp-Glu-Ala-Asp) box polypeptide 21a	H32543	0.99	0.721	1.42	0.000	1.28	0.015	1395316_at	*3
Ddx5	ddx5 gene	AA851926	0.91	0.052	1.31	0.004	1.23	0.027	1371837_at	
Ddx58_predicted	DEAD (Asp-Glu-Ala-Asp) box polypeptide 58 (predicted)	AI575264	0.54	0.007	1.74	0.009	1.43	0.014	1391463_at	
Dnch2	Dynein, cytoplasmic, heavy polypeptide 2	NM_023024	1.15	0.121	1.37	0.000	1.23	0.018	1368676_at	
Dnm1l	Dynamin 1–like	AI237251	0.82	0.091	1.56	0.006	1.62	0.022	1386460_x_at	
Entpd6	Ectonucleoside triphosphate diphosphohydrolase 6	NM_053498	1.28	0.060	0.78	0.017	0.80	0.044	1368315_at	
Gna11	Guanine nucleotide binding protein, alpha 11	NM_031033	0.91	0.060	0.81	0.025	0.80	0.042	1387822_at	
Gnai3	Guanine nucleotide binding protein, alpha inhibiting 3	J03219	1.13	0.303	1.64	0.007	1.20	0.042	1368030_at	
Ighmbp2	Immunoglobulin mu binding protein 2	NM_031586	0.88	0.112	0.79	0.009	0.81	0.048	1368855_at	
*1	Similar to macrophage migration inhibitory factor	AI170755	0.88	0.209	2.05	0.004	1.85	0.021	1388689_at	*2

Pcyox1	Prenylcysteine oxidase 1	AF332142	1.01	0.788	1.42	0.005	1.33	0.018	1370407_at
Pex6	Peroxisomal biogenesis factor 6	NM_057125	0.91	0.674	0.67	0.016	0.80	0.002	1368264_at
RGD1306100_predicted	Similar to RRP22 (predicted)	AI412866	0.84	0.021	0.75	0.010	0.78	0.029	1376909_at
Rhoj	Ras homolog gene family, member J	BM389644	0.91	0.289	1.54	0.018	1.27	0.035	1372835_at
Sept5	Septin 5	NM_053931	0.99	0.404	0.67	0.009	0.78	0.038	1367852_s_at
Tcirg1	T-cell, immune regulator 1, ATPase, H^+ transporting, lysosomal V0 protein a isoform 3	BM392376	0.89	0.031	1.57	0.014	1.24	0.003	1380019_at
Yme1l1	YME1 (*S. cerevisiae*)-like 1	AA849923	1.21	0.252	1.98	0.022	2.07	0.000	1385999_at

Protein serine/threonine kinase activity

Name	Description	Accession No.	Sham		OBX + Imipramine		OBX + SNC80		Probe	
			Fold change	*P*-value	Fold change	*P*-value	Fold change	*P*-value		
Acvr2a	Activin receptor IIA	BM383968	1.12	0.186	1.48	0.013	1.24	0.009	1381220_at	
Adrbk1	Adrenergic receptor kinase, beta 1	NM_012776	0.85	0.149	0.74	0.024	0.83	0.037	1387429_at	
Camk2b	Calcium/calmodulin-dependent protein kinase II beta subunit	NM_021739	1.04	0.264	0.63	0.001	0.80	0.006	1398251_a_at	
Cerk_predicted	Ceramide kinase (predicted)	AW525194	0.92	0.040	0.81	0.011	0.73	0.002	1375987_at	
Clk1	CDC-like kinase 1	AI177513	0.99	0.815	1.29	0.010	1.19	0.019	1399022_at	
Csnk2a2_predicted	Casein kinase II, alpha 2, polypeptide (predicted)	BI290750	1.30	0.021	0.71	0.019	0.82	0.039	1378282_at	
Dyrk3	Dual-specificity tyrosine-(Y)-phosphorylation regulated kinase 3	BI291080	0.96	0.396	1.28	0.049	1.43	0.028	1383650_at	*2
Epha7	Eph receptor A7	NM_134331	1.19	0.186	1.34	0.035	1.45	0.006	1369096_at	
Ephb3_predicted	Eph receptor B3 (predicted)	AW534949	1.13	0.729	0.71	0.007	0.80	0.032	1385788_at	
Hspb8	Heat shock 22kDa protein 8	NM_053612	1.01	0.992	1.46	0.005	1.25	0.047	1387282_at	
Kalrn	Kalirin, RhoGEF kinase	NM_032062	0.91	0.186	0.71	0.024	0.83	0.005	1368979_at	
Map4k3	Mitogen-activated protein kinase kinase kinase kinase 3	BG664160	1.06	0.754	1.33	0.014	1.28	0.045	1371042_at	
Pctk1	PCTAIRE-motif protein kinase 1	U36444	0.98	0.927	0.76	0.000	0.83	0.049	1370326_at	
Prkch	Protein kinase C-eta	AA799981	1.18	0.126	1.47	0.002	1.62	0.004	1388836_at	
Ripk1_predicted	Receptor (TNFRSF)-interacting serine-threonine kinase 1 (predicted)	BF289001	0.80	0.180	1.45	0.012	1.24	0.039	1371529_at	
Rock1	Rho-associated coiled-coil forming kinase 1	NM_031098	0.96	0.729	1.76	0.017	1.52	0.002	1368932_at	
Rock2	Rho-associated coiled-coil forming kinase 2	NM_013022	0.74	0.042	0.53	0.004	0.69	0.004	1387379_at	
Stk3	Serine/threonine kinase 3	NM_031735	0.86	0.010	1.52	0.004	1.22	0.005	1369712_at	
Tlk1_predicted	Tousled-like kinase 1 (predicted)	BG379991	1.04	0.496	1.31	0.004	1.31	0.001	1382114_at	

N-Acetyltransferase activity

Symbol	Descripiton	Accession No.	Sham		OBX + Imipramine		OBX + SNC80		Probe
			Fold change	*P*-value	Fold change	*P*-value	Fold change	*P*-value	
Cml1	Camello-like 1	NM_133558	0.88	0.036	1.44	0.014	1.41	0.001	1368208_at
Cml2	Camello-like 2	NM_021668	1.45	0.087	0.69	0.013	0.59	0.019	1368366_at
Cml3	Camello-like 3	AF187814	1.44	0.061	0.54	0.016	0.49	0.007	1370991_at
Crebbp	CREB binding protein	BF566908	0.88	0.245	0.46	0.008	0.73	0.008	1385852_at
Ogt	O-linked N-acetylglucosamine (GlcNAc) transferase (UDP-N-acetylglucosamine:polypeptide-N-acetylglucosaminyl transferase)	U76557	1.10	0.339	1.35	0.004	1.23	0.013	1370543_at

Protein modification process

Symbol	Description	Accession No.	Sham		OBX + Imipramine		OBX + SNC80		Probe
			Fold change	*P*-value	Fold change	*P*-value	Fold change	*P*-value	
Acvr2a	Activin receptor IIA	BM383968	1.12	0.186	1.48	0.013	1.24	0.009	1381220_at
Adrbk1	Adrenergic receptor kinase, beta 1	NM_012776	0.85	0.149	0.74	0.024	0.83	0.037	1387429_at
Asphd2	Aspartate beta-hydroxylase domain containing 2	BF412025	0.92	0.087	0.75	0.002	0.80	0.027	1395637_at
Ate1_predicted	Arginine-tRNA-protein transferase 1 (predicted)	BI276525	1.10	0.046	1.31	0.012	1.22	0.019	1377820_a_at
Cacybp	Calcyclin binding protein	BG664561	1.05	0.062	1.36	0.002	1.39	0.006	1392912_at
Cacybp	Calcyclin binding protein	AW918443	1.11	0.235	1.31	0.004	1.29	0.028	1392979_at
Camk2b	Calcium/calmodulin-dependent protein kinase II beta subunit	NM_021739	1.04	0.264	0.63	0.001	0.80	0.006	1398251_a_at
Commd7	COMM domain containing 7	BG375350	1.04	0.318	0.76	0.003	0.82	0.003	1388400_at
Csnk2a2_predicted	Casein kinase II, alpha 2, polypeptide (predicted)	BI290750	1.30	0.021	0.71	0.019	0.82	0.039	1378282_at
Gna11	Guanine nucleotide binding protein, alpha 11	NM_031033	0.91	0.060	0.81	0.025	0.80	0.042	1387822_at
Herc4	Hect domain and RLD 4	AI236889	1.02	0.431	1.32	0.018	1.27	0.015	1373381_at
Jak3	Janus kinase 3	NM_012855	0.68	0.122	1.89	0.002	1.34	0.017	1368251_at
Kalrn	Kalirin, RhoGEF kinase	NM_032062	0.91	0.186	0.71	0.024	0.83	0.005	1368979_at
Kitl	Kit ligand	BG374178	0.87	0.133	0.76	0.022	0.75	0.004	1388856_at
Kitl	Kit ligand	BF562720	0.88	0.420	1.19	0.038	0.77	0.028	1396214_at
LOC687633	Similar to ubiquitin protein ligase E3B	BF281133	0.95	0.195	0.71	0.002	0.81	0.000	1371728_at
Man1a_predicted	Mannosidase 1, alpha (predicted)	AA892549	1.05	0.227	1.42	0.007	1.24	0.005	1371988_at
Man1c1_predicted	Mannosidase, alpha, class 1C, member 1 (predicted)	AI179443	1.03	0.925	1.54	0.011	1.25	0.010	1393053_at
Map4k3	Mitogen-activated protein kinase kinase kinase kinase 3	BG664160	1.06	0.754	1.33	0.014	1.28	0.045	1371042_at
Mgat2	Mannoside acetylglucosaminyltransferase 2	NM_053604	1.06	0.242	1.55	0.000	1.40	0.003	1386982_at
Msra	Methionine sulfoxide reductase A	NM_053307	1.24	0.018	0.63	0.036	0.70	0.016	1387531_at
Mvk	Mevalonate kinase	AW433971	1.01	0.886	0.63	0.029	0.78	0.006	1387119_at
Ogt	O-linked N-acetylglucosamine (GlcNAc) transferase (UDP-N-acetyl-glucosamine:polypeptide-N-acetylglucosaminyl transferase)	U76557	1.10	0.339	1.35	0.004	1.23	0.013	1370543_at
Pcmtd2_predicted	Protein-L-isoaspartate (D-aspartate) O-methyltransferase domain containing 2 (predicted)	BM388557	0.96	0.378	1.43	0.010	1.38	0.000	1374454_at
Pctk1	PCTAIRE-motif protein kinase 1	U36444	0.98	0.927	0.76	0.000	0.83	0.049	1370326_at
Pias4	Protein inhibitor of activated STAT, 4	AI412927	0.96	0.467	0.71	0.007	0.81	0.015	1398352_at
Pigq	Phosphatidylinositol glycan, class Q	BF288309	1.03	0.837	0.75	0.017	0.77	0.014	1392687_at
Pik3ca	Phosphatidylinositol 3-kinase, catalytic, alpha polypeptide	AA964375	0.89	0.321	1.55	0.002	1.48	0.001	1393499_at
Ppm1b	Protein phosphatase 1B, magnesium dependent, beta isoform	AI501282	0.73	0.013	1.29	0.017	1.27	0.042	1378124_at
Ppp1cb	Protein phosphatase 1, catalytic subunit, beta isoform	NM_013065	0.89	0.496	1.57	0.000	1.55	0.002	1386950_at
Prkch	Protein kinase C-eta	AA799981	1.18	0.126	1.47	0.002	1.62	0.004	1388836_at

Ptp4a1	Protein tyrosine phosphatase 4a1	AI172261	1.15	0.010	1.27	0.000	1.35	0.001	1370193_at
Ptpn3	Protein tyrosine phosphatase, non-receptor type 3	AI317821	0.93	0.122	0.77	0.012	0.78	0.029	1389362_at
Ptprr	Protein tyrosine phosphatase, receptor type, R	NM_053594	1.06	0.454	1.20	0.008	1.33	0.000	1368358_a_at
Rbx1	Ring-box 1	AI179646	0.83	0.092	1.43	0.012	1.35	0.016	1388538_at
RGD1304758	Similar to RIKEN cDNA 2010008E23 gene	AI412948	1.01	0.976	0.76	0.010	0.79	0.002	1373244_at
RGD1310090	Similar to 2310043K02Rik protein	BI291423	1.04	0.745	0.74	0.009	0.76	0.009	1372359_at
RGD1310450	Similar to hypothetical protein	AI500903	1.06	0.774	1.38	0.035	1.27	0.011	1396842_at
Rnf138	Ring finger protein 138	AW529177	1.23	0.223	1.45	0.009	1.35	0.033	1382379_at
Rock1	Rho-associated coiled-coil forming kinase 1	NM_031098	0.96	0.729	1.76	0.017	1.52	0.002	1368932_at
Rock2	Rho-associated coiled-coil forming kinase 2	NM_013022	0.74	0.042	0.53	0.004	0.69	0.004	1387379_at
Sbf1_predicted	SET binding factor 1 (predicted)	AW434982	0.91	0.493	0.75	0.009	0.79	0.036	1377174_at
Stk3	Serine/threonine kinase 3	NM_031735	0.86	0.010	1.52	0.004	1.22	0.005	1369712_at
Tlk1_predicted	Tousled-like kinase 1 (predicted)	BG379991	1.04	0.496	1.31	0.004	1.31	0.001	1382114_at
Ubadc1	Ubiquitin associated domain containing 1	BI275880	1.06	0.269	0.83	0.030	0.82	0.009	1388387_at
Ubc2e	Ubiquitin-conjugating enzyme E2D 2	AW142720	1.03	0.966	1.64	0.008	1.45	0.019	1370523_a_at

Regulation of cellular process

Symbol	Description	Accession No.	Sham		OBX + Imipramine		OBX + SNC80		Probe	
			Fold change	*P*-value	Fold change	*P*-value	Fold change	*P*-value		
Adrbk1	Adrenergic receptor kinase, beta 1	NM_012776	0.85	0.149	0.74	0.024	0.83	0.037	1387429_at	
Api5_predicted	Apoptosis inhibitor 5 (predicted)	H34636	1.05	0.583	1.57	0.017	1.50	0.002	1395894_at	
Bbc3	Bcl-2 binding component 3	AI236152	1.16	0.483	1.60	0.014	1.32	0.015	1382993_at	
Bcl2l1	Bcl2-like 1	AF279286	1.08	0.971	0.69	0.041	0.69	0.049	1370485_a_at	
Btg3	B-cell translocation gene 3	NM_019290	1.37	0.025	1.48	0.020	1.32	0.015	1368072_at	
Cacna1a	Calcium channel, voltage-dependent, P/Q type, alpha 1A subunit	AF051527	0.85	0.294	0.64	0.019	0.65	0.031	1386939_a_at	
Cav2	Caveolin 2	NM_131914	1.07	0.632	1.67	0.013	1.46	0.003	1370135_at	
Ccnl2	Cyclin L2	AA892159	0.87	0.236	1.24	0.016	1.21	0.042	1389564_at	
Cd38	CD38 antigen	BI289418	1.10	0.009	1.65	0.004	1.34	0.031	1390325_at	
Centg3_predicted	Centaurin, gamma 3 (predicted)	AW252124	0.80	0.284	0.62	0.044	0.69	0.022	1376499_at	
Chd6_predicted	Chromodomain helicase DNA binding protein 6 (predicted)	BF398050	0.87	0.302	1.37	0.048	1.36	0.025	1379580_at	
Cic_predicted	Capicua homolog (Drosophila) (predicted)	AI029769	0.98	0.977	0.71	0.003	0.73	0.012	1382322_a_at	
Cml2	Camello-like 2	NM_021668	1.45	0.087	0.69	0.013	0.59	0.019	1368366_at	
Cml3	Camello-like 3	AF187814	1.44	0.061	0.54	0.016	0.49	0.007	1370991_at	
Cnot7_predicted	CCR4-NOT transcription complex, subunit 7 (predicted)	BE111850	0.95	0.632	1.23	0.001	1.31	0.003	1367515_at	
Crebbp	CREB binding protein	BF566908	0.88	0.245	0.46	0.008	0.73	0.008	1385852_at	
Csnk2a2_predicted	Casein kinase II, alpha 2, polypeptide (predicted)	BI290750	1.30	0.021	0.71	0.019	0.82	0.039	1378282_at	
Cx3cl1	Chemokine (C-X3-C motif) ligand 1	NM_134455	1.09	0.409	0.68	0.001	0.76	0.011	1368200_at	
Dapk3	Death-associated protein kinase 3	AI029121	0.97	0.466	1.41	0.009	1.51	0.043	1383448_at	*4
Ddx5	ddx5 gene	AA851926	0.91	0.052	1.31	0.004	1.23	0.027	1371837_at	
Dio2	Deiodinase, iodothyronine, type II	NM_031720	1.13	0.215	0.77	0.015	0.81	0.014	1387103_s_at	*5
Dlc1	Deleted in liver cancer 1	AI176713	0.98	0.251	0.82	0.008	0.81	0.017	1373291_at	
Egr1	Early growth response 1	NM_012551	1.19	0.162	0.80	0.035	0.68	0.004	1368321_at	
Egr4	Early growth response 4	NM_019137	1.54	0.001	0.78	0.035	0.71	0.011	1387442_at	
Fmr1	Fragile X mental retardation syndrome 1 homolog	AI705393	0.93	0.288	1.25	0.047	1.26	0.006	1393459_at	
Gabpa_predicted	GA repeat binding protein, alpha (predicted)	BG372192	0.85	0.058	1.77	0.001	1.43	0.001	1383377_at	
Gna11	Guanine nucleotide binding protein, alpha 11	NM_031033	0.91	0.060	0.81	0.025	0.80	0.042	1387822_at	
Gpsm1	G-protein signalling modulator 1 (AGS3-like, *C. elegans*)	AW435429	1.01	0.191	1.23	0.003	1.21	0.007	1372383_at	
Havcr2	Hepatitis A virus cellular receptor 2	BF399036	1.05	0.435	1.43	0.009	1.22	0.011	1377263_at	*2
Hdac4_predicted	Histone deacetylase 4 (predicted)	BF419085	0.88	0.107	0.79	0.003	0.74	0.009	1376761_at	
Homer1	HS1 binding protein	AB003726	0.79	0.119	0.54	0.001	0.48	0.040	1370454_at	
Homer1	HS1 binding protein	AF030088	1.41	0.272	0.46	0.001	0.32	0.004	1370997_at	
Hsd3b7	Hydroxy-delta-5-steroid dehydrogenase, 3 beta- and steroid delta-isomerase 7	AB000199	0.91	0.444	1.21	0.019	1.22	0.013	1370433_at	
Ift88_predicted	Intraflagellar transport 88 homolog (Chlamydomonas) (predicted)	AI547895	1.01	0.505	1.24	0.012	1.26	0.002	1384915_at	
Ighmbp2	Immunoglobulin mu binding protein 2	NM_031586	0.88	0.112	0.79	0.009	0.81	0.048	1368855_at	
Ing1	Inhibitor of growth family, member 1	AI170649	0.99	0.020	0.83	0.023	0.83	0.006	1373457_at	
Jak3	Janus kinase 3	NM_012855	0.68	0.122	1.89	0.002	1.34	0.017	1368251_at	
Kcnh1	Potassium voltage-gated channel, subfamily H (eag-related), member 1	NM_031742	1.06	0.224	0.78	0.002	0.76	0.020	1368061_at	
Khsrp	KH-type splicing regulatory protein	BI295086	0.89	0.303	0.57	0.002	0.75	0.043	1375426_a_at	
Kitl	Kit ligand	BG374178	0.87	0.133	0.76	0.022	0.75	0.004	1388856_at	
Limd1_predicted	LIM domains containing 1 (predicted)	BI289676	0.92	0.673	1.46	0.001	1.26	0.020	1372668_at	
LOC497729	Hypothetical gene supported by NM_172157	AI412401	0.83	0.047	1.25	0.031	1.37	0.019	1381925_x_at	
LOC499900	Similar to Zinc finger protein 133	AI146063	1.25	0.076	1.25	0.001	1.41	0.035	1389709_at	
Madd	MAP-kinase activating death domain	NM_053585	0.97	0.292	0.77	0.001	0.74	0.013	1369066_at	
Mina	Myc induced nuclear antigen	BI278157	0.98	0.973	1.36	0.001	1.22	0.009	1392743_at	
Mrps31_predicted	Mitochondrial ribosomal protein S31 (predicted)	AI171229	1.01	0.909	0.83	0.025	0.80	0.010	1372456_at	
Mtap2	Microtubule-associated protein 2	X74211	0.91	0.417	0.57	0.009	0.78	0.028	1368411_a_at	
Mvk	Mevalonate kinase	AW433971	1.01	0.886	0.63	0.029	0.78	0.006	1387119_at	
Myt1_predicted	Myelin transcription factor 1 (predicted)	AI070390	1.20	0.331	1.41	0.004	1.53	0.029	1392332_at	
Ngfrap1	Nerve growth factor receptor (TNFRSF16) associated protein 1	BG381021	0.89	0.103	1.32	0.018	1.22	0.026	1385534_at	
Pacsin1	Protein kinase C and casein kinase substrate in neurons 1	NM_017294	0.92	0.280	0.56	0.006	0.80	0.034	1368958_at	
Phf12	PHD finger protein 12	AA924840	1.02	0.818	1.49	0.009	1.49	0.003	1394014_at	
Pias4	Protein inhibitor of activated STAT, 4	AI412927	0.96	0.467	0.71	0.007	0.81	0.015	1398352_at	
Pik3ca	Phosphatidylinositol 3-kinase, catalytic, alpha polypeptide	AA964375	0.89	0.321	1.55	0.002	1.48	0.001	1393499_at	
Pnrc1	Proline rich 2	U61729	1.07	0.040	1.44	0.000	1.21	0.046	1370381_at	
Pspc1	Paraspeckle protein 1	AI136693	0.96	0.676	1.45	0.011	1.52	0.010	1384465_at	
Pycard	PYD and CARD domain containing	BI282953	0.64	0.052	1.77	0.004	1.31	0.044	1389873_at	
Rasa1	RAS p21 protein activator 1	BG668164	1.03	0.757	1.57	0.000	1.34	0.010	1393173_at	
Rbbp9	Retinoblastoma-binding protein 9	AA956258	0.89	0.206	1.45	0.002	1.35	0.007	1394033_at	
Ripk1_predicted	Receptor (TNFRSF)-interacting serine-threonine kinase 1 (predicted)	BF289001	0.80	0.180	1.45	0.012	1.24	0.039	1371529_at	
Rock1	Rho-associated coiled-coil forming kinase 1	NM_031098	0.96	0.729	1.76	0.017	1.52	0.002	1368932_at	
Runx1t1	Runt-related transcription factor 1; translocated to, 1 (cyclin D-related)	BE105678	0.78	0.006	1.42	0.006	1.55	0.004	1385519_at	

Runx1t1	Runt-related transcription factor 1; translocated to, 1 (cyclin D-related)	BF408914	1.05	0.293	0.53	0.029	0.61	0.035	1393901_at	
Sbf1_predicted	SET binding factor 1 (predicted)	AW434982	0.91	0.493	0.75	0.009	0.79	0.036	1377174_at	
Scap_predicted	SREBP cleavage activating protein (predicted)	AI145323	0.98	0.715	1.41	0.030	1.33	0.045	1384464_at	
Sec14l2	SEC14-like 2 (*S. cerevisiae*)	AI575603	1.00	0.702	0.75	0.032	0.80	0.026	1374308_at	
Sept5	Septin 5	NM_053931	0.99	0.404	0.67	0.009	0.78	0.038	1367852_s_at	
Sh3md2	Putative scaffolding protein POSH	BG372003	0.98	0.503	1.70	0.033	1.50	0.026	1397620_at	
Slc12a4	Solute carrier family 12, member 4	NM_019229	0.77	0.090	2.02	0.006	1.26	0.041	1368125_at	
Snx17	Sorting nexin 17	BE329329	0.95	0.292	0.81	0.027	0.82	0.000	1373061_at	
Sphk2	Sphingosine kinase 2	AI716502	0.96	0.518	1.54	0.036	1.43	0.027	1376216_at	
Stim1_predicted	Stromal interaction molecule 1 (predicted)	BI292282	0.98	0.732	0.70	0.002	0.80	0.011	1382121_at	
Stk3	Serine/threonine kinase 3	NM_031735	0.86	0.010	1.52	0.004	1.22	0.005	1369712_at	
Taf9l	TAF9-like RNA polymerase II, TATA box binding protein (TBP)-associated factor, 31 kDa	NM_133615	1.03	0.690	1.21	0.036	1.33	0.005	1368429_at	
Tcfcp2_predicted	Transcription factor CP2 (predicted)	AW527419	0.96	0.653	1.58	0.000	1.67	0.000	1378218_at	
Tgfb2	Transforming growth factor, beta 2	NM_031131	0.91	0.388	1.44	0.007	1.24	0.001	1387172_a_at	
Thoc1	THO complex 1	BM384228	0.92	0.187	1.22	0.010	1.37	0.016	1376641_at	
Tlk1_predicted	Tousled-like kinase 1 (predicted)	BG379991	1.04	0.496	1.31	0.004	1.31	0.001	1382114_at	
Tmod1	Tropomodulin 1	AI104913	1.28	0.022	0.73	0.004	0.75	0.004	1388718_at	
Txnl1	Thioredoxin-like 1	BF555110	1.04	0.101	1.22	0.005	1.21	0.006	1380191_s_at	
Ubtf	Upstream binding transcription factor, RNA polymerase I	AI105117	0.99	0.894	0.76	0.001	0.81	0.009	1389830_at	
Vipr1	Vasoactive intestinal peptide receptor 1	BI301509	0.94	0.512	0.69	0.035	0.78	0.028	1383695_at	
Zfhx1b	Zinc finger homeobox 1b	AW529031	0.84	0.487	1.36	0.016	1.26	0.014	1390940_at	
Zfhx1b	Zinc finger homeobox 1b	BG377397	0.79	0.778	1.43	0.005	1.91	0.004	1393795_at	*6
Zfp131	Zinc finger protein 131	AA924380	0.99	0.520	1.67	0.008	1.51	0.012	1393780_at	
Zfp446_predicted	Zinc finger protein 446 (predicted)	BM389392	1.03	0.569	1.35	0.030	1.22	0.009	1391702_at	
Zfp61	Zinc finger protein 61	AI030120	0.90	0.534	1.22	0.012	1.33	0.030	1398663_at	
Znf386	Zinc finger protein 386 (Kruppel-like)	NM_019620	0.82	0.066	1.43	0.014	1.25	0.044	1368712_at	

Regulation of neurotransmitter levels

Symbol	Description	Accession No.	Sham		OBX + Imipramine		OBX + SNC80		Probe	
			Fold change	*P*-value	Fold change	*P*-value	Fold change	*P*-value		
Glul	Glutamate-ammonia ligase (glutamine synthase)	BM386267	1.00	0.473	0.80	0.038	0.75	0.015	1375569_at	
Hnmt	Histamine N-methyltransferase	NM_031044	1.06	0.821	1.32	0.040	1.44	0.004	1387382_at	
Sec10l1	Sec10-like 1 (*S. cerevisiae*)	BF386083	1.04	0.790	1.68	0.004	1.42	0.005	1395155_at	*7
Sept5	Septin 5	NM_053931	0.99	0.404	0.67	0.009	0.78	0.038	1367852_s_at	
Slc1a3	Solute carrier family 1 (glial high affinity glutamate transporter), member 3	X63744	0.81	0.449	1.34	0.011	1.43	0.047	1371130_at	
Stx1a	Syntaxin 1A (brain)	NM_053788	0.99	0.769	0.71	0.009	0.78	0.038	1387359_at	
Syt12	Synaptotagmin XII	AW527241	1.04	0.093	0.67	0.001	0.77	0.018	1398099_at	*2
Tgfb2	Transforming growth factor, beta 2	NM_031131	0.91	0.388	1.44	0.007	1.24	0.001	1387172_a_at	
Unc13c	Unc-13 homolog C (*C. elegans*)	U75361	0.85	0.121	0.71	0.045	0.70	0.017	1370546_at	

*1: no symbol, *2: no assignment symbol and description by NetAffx, *3: assign Mageh1 (melanoma antigen, family H, 1) by NetAffx, *4: assign Irf9 (interferon regulatory factor 9) by NetAffx, *5: assign Slc25a14 (solute carrier family 25, member 14) by NetAffx, *6: assign Zeb2 (zinc finger E-box binding homeobox 2) by NetAffx, *7: assign Exoc5 (exocyst complex component 5) by NetAffx.

tion of the genes affected by imipramine and SNC80 treatment. Table 2 lists differentially expressed genes identified according to selected enriched gene ontology terms. Figure 4 showed the systematic scheme of Table 1.

Discussion

In the present study, chronic administration of imipramine or SNC80 significantly reduced hyper-emotionality in OBX rats (Fig. 1). The changes of emotional response were consistent with our previous report (21).

On the other hand, we have previously performed several behavioral experiments including the elevated plus maze test in OBX rats (21, 30). OBX rats showed a decrease of the time spent and the number of entries in the open arm of a plus-maze test with vehicle treatment for 7 days, and a recovery of those with treatment of SNC80 and desipramine (21). Thus, the molecular systems affected by imipramine and SNC80 treatment in OBX rats may also be related to antianxiety-like action in addition to antidepressant-like action.

In the frontal cortex, glucose metabolism, blood flow, and electroencephalograph activity are altered in depressed patients (31). Thus, we analyzed frontal cortex samples in this study. However, it is necessary to examine the gene expression profile in the hippocampus and other related brain structures in future.

Gene expression analysis can be used to explain the effects of drugs. Hierarchical cluster analysis can reveal drug action characteristics and thus can be used to estimate the differences and similarities in the actions of various drugs. In the present study, we used gene expression analysis to determine the mechanisms of action of two drugs, imipramine and SNC80, in an animal model of depression. Hierarchical clustering analysis of gene expression data assigned samples from the same drug treatment group into a single cluster (Fig. 2), indicating these samples shared similar gene expression patterns. Indeed, we found that gene expression patterns were similar in OBX rats treated chronically with the antidepressant imipramine and those

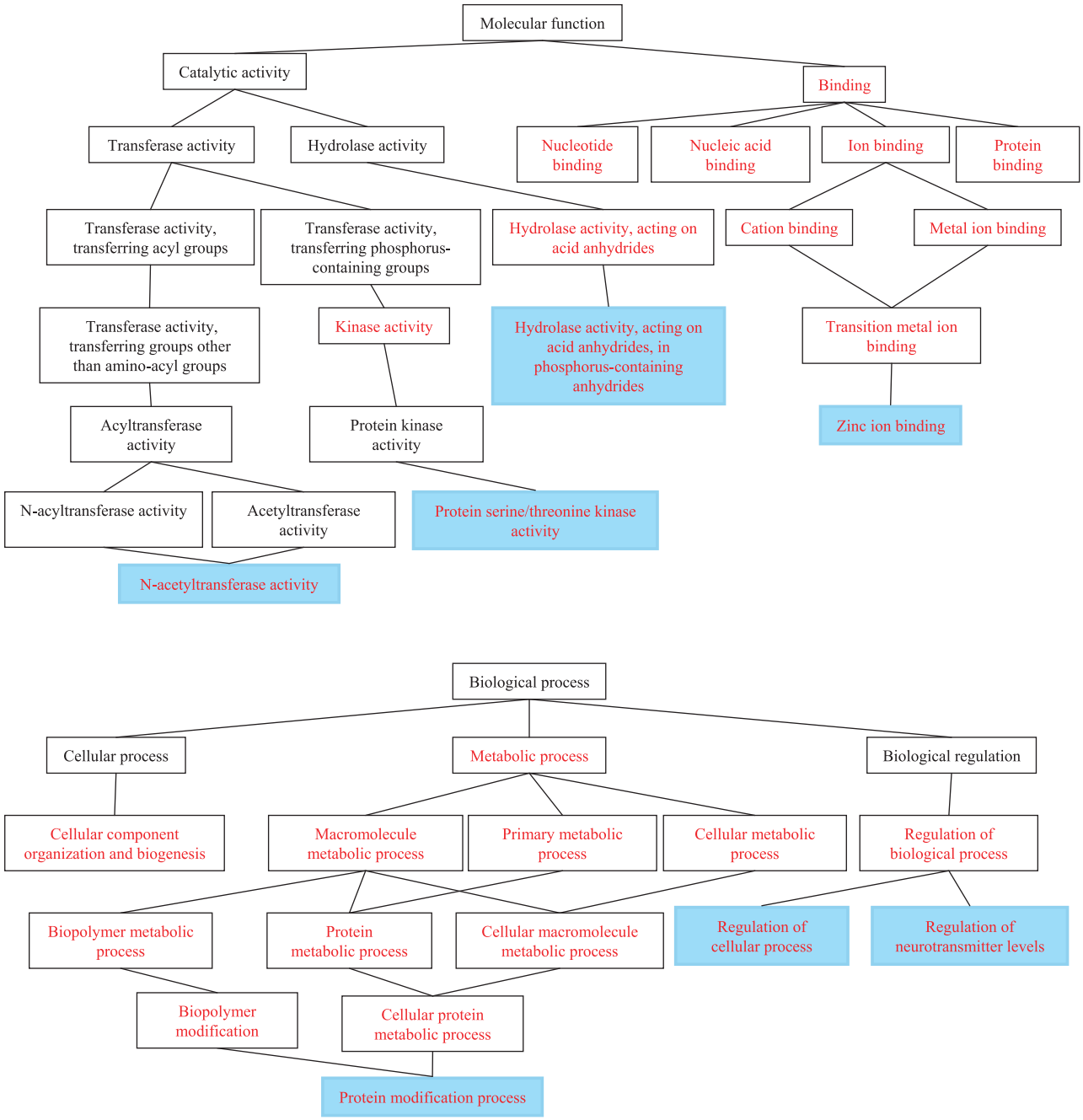

Fig. 4. Functional clustering of the genes affected by imipramine and SNC80 treatment. Biological/functional classifications are organized according to GO pathways, which are linked as hierarchical clusters, with the most general function positioned at a primary node and more specific functions positioned at subsequent nodes. The red characters indicate the functional classifications, which showed statistical significance of association between the 577 genes and GO database ($P<0.01$). Differentially expressed genes identified according to selected enriched gene ontology terms (highlighted in blue) are shown in Table 2.

treated chronically with the delta-opioid agonist SNC80. This is consistent with findings from primary cultures treated in vitro with CNS acting drugs (opioids, antidepressants, and antipsychotic drugs) (32). Microarray analysis of these cells showed that the gene expression profile of cells treated with antidepressants was similar to that of cells treated with a delta-opioid agonist.

The similarity in the effects of imipramine and SNC80 on gene expression was also seen when significant changes in gene expression were analyzed further (Fig. 3). A total of 577 genes were significantly affected by imipramine and SNC80 treatment. Of the 577 genes,

only 3 genes responded oppositely to imipramine and SNC80 treatment (Fig. 3e), suggesting that the CNS functions affected by these drugs were more similar than dissimilar. Interestingly, 35 genes responded to drug treatment by adjusting their expression levels to that of the sham (Fig. 3c). Taken together, our findings indicate that in OBX rats the mechanisms underlying drug action differ from those mediating emotional changes. In the clinical situation, the pathogenic development of depression may be different from the mechanism of antidepressant action.

The elucidation of the mechanisms that direct antidepressant actions should be approached from the viewpoint of the CNS as a whole. One such approach is based on the analysis of a large number of gene expression changes. To date, antidepressants have been reported to affect the expression of many immediate early genes and transcription factors. These regulatory proteins induce many changes in the expression of downstream genes. GeneChip® technology has proven to be very useful for analyzing a large number of genes. However, replicating gene expression data has been problematic. The reproducibility of microarray techniques has been evaluated by way of laboratory correlations and different platform correlations (cDNA microarrays and oligonucleotide chips). These studies showed that gene-by-gene comparisons show exceedingly poor correlation among platforms and across laboratories (33 – 38). However, the reproducibility improved substantially when microarray analysis was based on commonly accepted biological GO terms as opposed to analysis based on gene-by-gene comparisons (35). Consequently, we analyzed mechanisms underlying antidepressant actions based on functional classes rather than on individual gene comparisons. Identifying the functional classes that are affected by antidepressants would lead to the identification of candidate neuronal systems affected by antidepressant treatments. It will be necessary to analyze the individual gene expression changes in future studies.

On the basis of the above analysis schema, we identified common functional changes induced by imipramine and SNC 80 in OBX rats. Using the GO database, we also related the changes we observed in gene expression to specific functions, which included zinc ion binding; hydrolase activity, acting on acid anhydrides, in phosphorus-containing anhydrides; protein serine/threonine kinase activity; N-acetyltransferase activity; protein modification process; regulation of cellular process; and regulation of neurotransmitter levels.

We examined the gene expression analysis at 24 h after the last drug administration to exclude possible acute effects by the drug treatments. However, it is difficult to distinguish antidepressant-like effects from withdrawal effects. In the future, it will be necessary to make clear which functional classes are important for recovery of depressed patients.

Zinc ion binding

During the last several years, important roles of zinc in the psychopathology and therapy of depression have been identified. Recently, clinical data have revealed lower serum zinc concentration in depressed patients (39, 40). Clinical studies have shown zinc supplementation to be beneficial in the antidepressant therapy of depressed patients (41). Zinc also exhibits antidepressant-like effects in behavioral tests and models used to evaluate antidepressant activity, such as the forced swim test and tail suspension test (42 – 44), and in olfactory bulbectomy, chronic mild stress (CMS), and chronic unpredictable stress (CUS) animal models of depression (45 – 47). A recent study demonstrated that acute and chronic treatment with zinc has antidepressant-like effects in OBX rats tested in a passive avoidance task (45). Zinc also significantly decreased the time of walking and number of rearing and peeping in the OBX rats (45). Moreover, chronic zinc treatment reversed the CMS-induced reduction in the consumption of 1% sucrose solution by rats (46). Recently, prolonged zinc treatment has been shown to prevent a deficit in fighting behavior in rats in the CUS model (47). Moreover, in the same model, zinc supplementation potentiated the antidepressant effects of imipramine (47). All of these animal data strongly suggest that zinc possesses possible antidepressant activity.

Hydrolase activity, acting on acid anhydrides, in phosphorus-containing anhydrides

Genes encoding proteins that participate in the hydrolysis of phosphorus-containing acid anhydrides are thought to be involved in various brain functions. Therefore, it is difficult to ascertain the specific action of antidepressants based on this category. However, many genes assigned to this category are related to the ATP-binding cassette (ABC) transporter, which regulates the concentration of drugs in the CNS. Antidepressants are reportedly effluxed from the CNS by the ABC transporter (48, 49). In addition, various antidepressant compounds are differentially recognized as substrates for the ABC transporter (48, 49), and certain substrates such as St. John's wort, a known herbal antidepressant, increase the expression and function of the ABC transporter (50, 51). Indeed, antidepressants may affect ABC transporter activity, thus regulating permeability of the blood brain barrier itself.

Protein serine/threonine kinase activity, protein modification process, and regulation of cellular process

Because genes encoding proteins involved in protein serine/threonine kinase activity, protein modification, or regulation of cellular process have diverse functions, it is difficult to identify the specific actions of antidepressants on the basis of these categories. Each category contained many axonal/dendritic-related genes, N-glycan biosynthesis–related genes, and signal transduction-related genes. However, the present study did not determine the specific function of the genes in the CNS. Further studies are needed.

N-Acetyltransferase activity

A gene that is related to N-acetyltransferase activity has been reported to be involved in antidepressant actions. Serotonin N-acetyltransferase catalyzes the rate-limiting step in the biosynthesis of the circadian hormone melatonin from serotonin. Chronic but not acute fluoxetine administration increases the expression of serotonin N-acetyltransferase in the prefrontal cortex and the hippocampus (52, 53).

This category also contained the Camello protein family and O-GlcNAc transferase protein. Camello proteins, which are localized in the Golgi complex, inhibit gastrulation in *Xenopus laevis*. Camello proteins participate in the acetylation of sugar residues in glycoproteins (54). O-GlcNAc transferase catalyzes the addition of a single N-acetylglucosamine to proteins. Therefore, antidepressants may affect N-acetyltransferase–regulated biosynthesis, especially the modification of glycoproteins.

Regulation of neurotransmitter levels

Antidepressants may regulate neurotransmitter levels, especially glutamate levels, in the synaptic cleft via regulation of exocytosis machinery and uptake machinery. Some clinical studies suggest that the glutamatergic system in depressed patients is pathological. For example, plasma and cerebrospinal fluid glutamate levels and glutamate/glutamine ratios are altered in depressed patients (55 – 57). More recent proton magnetic resonance spectroscopic analyses have identified alterations in glutamate levels in the anterior cingulate cortex and occipital cortex of depressed patients (58, 59). In addition, decreases in glial cell densities observed in depressed patients (60 – 62) may result in decreased glial glutamate transporter expression, thereby reducing the capacity to regulate synaptic concentrations of glutamate. Indeed, one microarray study suggested that glial glutamate transporter expression is decreased in the anterior cingulate cortex and dorsolateral prefrontal cortex of depressed patients (63). Glutamate uptake by glia is the primary mechanism for clearing glutamate from the synaptic cleft. Therefore, a glial deficit may contribute to glutamate hyperactivity in depressed patients.

The inhibition of glutamate release by antidepressant treatment has been reported. Two different drugs (imipramine and phenelzine) were found to reduce depolarization-evoked glutamate overflow from slices of prefrontal cortex after both acute and chronic treatment (64). Acute exposure to fluoxetine reduces depolarization-evoked glutamate release from cerebrocortical synaptosomes in vitro via inhibition of P/Q-type Ca^{2+} channels (65). Chronic antidepressant treatment suppresses depolarization-evoked release of glutamate from hippocampal synaptosomes, by reducing syntaxin-1/CaM kinase II interaction, activity that promotes neurotransmitter release. This treatment also increases syntaxin-1/Munc-18 interaction, an activity that reduces neurotransmitter release (66).

In the present study, we identified an astrocyte-expressed gene that regulates glutamate levels (Glul, Slc1a3). Previously, we also found an astrocyte-expressed gene, Ndrg2, whose expression was decreased by antidepressant treatments in the frontal cortex (67). These results suggest that antidepressants affect not only genes expressed by neurons but also by genes expressed by astrocytes. One of the antidepressant actions may regulate glutamate homeostasis via astrocytes.

Conclusions

In the present study, comprehensive gene expression analyses showed that two drugs with different mechanisms of action affected common neuronal systems in the frontal cortex of OBX rats. Defining the roles of these candidate neuronal systems in antidepressant-induced neural changes is likely to transform the course of research on the biological basis of mood disorders. Such detailed knowledge will have profound effects on the diagnosis, prevention, and treatment of depression.

Acknowledgments

This work was supported in part by Health Science Research Grants from the Japanese Ministry of Health, Labour, and Welfare and the Japanese Ministry of Education, Culture, Sport, Science, and Technology. We thank Dr Keiji Wada and Mr. Naoki Takagaki for the helpful discussions.

References

1 Yamada M, Higuchi T. Functional genomics and depression research. Beyond the monoamine hypothesis. Eur Neuro-

psychopharmacol. 2002;12:235–244.
2 Wong ML, O'Kirwan F, Hannestad JP, Irizarry KJ, Elashoff D, Licinio J. St John's wort and imipramine-induced gene expression profiles identify cellular functions relevant to antidepressant action and novel pharmacogenetic candidates for the phenotype of antidepressant treatment response. Mol Psychiatry. 2004;9: 237–251.
3 Conti B, Maier R, Barr AM, Morale MC, Lu X, Sanna PP, et al. Region-specific transcriptional changes following the three antidepressant treatments electro convulsive therapy, sleep deprivation and fluoxetine. Mol Psychiatry. 2007;12:167–189.
4 Kelly JP, Wrynn AS, Leonard BE. The olfactory bulbectomized rat as a model of depression: an update. Pharmacol Ther. 1997;74:299–316.
5 Song C, Leonard BE. The olfactory bulbectomised rat as a model of depression. Neurosci Biobehav Rev. 2005;29:627–647.
6 Thorne BM, Rowles JS. Memory deficit in passive-avoidance learning in bulbectomized Long-Evans hooded rats. Physiol Behav. 1988;44:339–345.
7 Redmond AM, Kelly JP, Leonard BE. Behavioural and neurochemical effects of dizocilpine in the olfactory bulbectomized rat model of depression. Pharmacol Biochem Behav. 1997;58: 355–359.
8 Okuyama S, Chaki S, Kawashima N, Suzuki Y, Ogawa S, Nakazato A, et al. Receptor binding, behavioral, and electrophysiological profiles of nonpeptide corticotropin-releasing factor subtype 1 receptor antagonists CRA1000 and CRA1001. J Pharmacol Exp Ther. 1999;289:926–935.
9 Ho YJ, Chen KH, Tai MY, Tsai YF. MK-801 suppresses muricidal behavior but not locomotion in olfactory bulbectomized rats: involvement of NMDA receptors. Pharmacol Biochem Behav. 2004;77:641–646.
10 Ho Y, Liu T, Tai M, Wen Z, Chow RS, Tsai Y, et al. Effects of olfactory bulbectomy on NMDA receptor density in the rat brain. Brain Res. 2001;900:214–218.
11 Bilkei-Gorzo A, Racz I, Michel K, Zimmer A. Diminished anxiety- and depression-related behaviors in mice with selective deletion of the Tac1 gene. J Neurosci. 2002;22:10046–10052.
12 Hong KW, Lee WS, Rhim BY. Role of central alpha 2-adrenoceptors on the development of muricidal behavior in olfactory bulbectomized rats: effect of alpha 2-adrenoceptor antagonists. Physiol Behav. 1987;39:535–539.
13 Jesberger JA, Richardson JS. Animal models of depression: parallels and correlates to severe depression in humans. Biol Psychiatry. 1985;20:764–784.
14 Willner P, Mitchell PJ. The validity of animal models of predisposition to depression. Behav Pharmacol. 2002;13:169–188.
15 van Riezen H, Leonard BE. Effects of psychotropic drugs on the behavior and neurochemistry of olfactory bulbectomized rats. Pharmacol Ther. 1990;47:21–34.
16 Cryan JF, McGrath C, Leonard BE, Norman TR. Combining pindolol and paroxetine in an animal model of chronic antidepressant action--can early onset of action be detected? Eur J Pharmacol. 1998;352:23–28.
17 Redmond AM, Kelly JP, Leonard BE. The determination of the optimal dose of milnacipran in the olfactory bulbectomized rat model of depression. Pharmacol Biochem Behav. 1999;62:619–623.
18 Mochizuki D, Tsujita R, Yamada S, Kawasaki K, Otsuka Y, Hashimoto S, et al. Neurochemical and behavioural characterization of milnacipran, a serotonin and noradrenaline reuptake inhibitor in rats. Psychopharmacology (Berl). 2002;162:323–332.
19 Wieronska JM, Papp M, Pilc A. Effects of anxiolytic drugs on some behavioral consequences in olfactory bulbectomized rats. Pol J Pharmacol. 2001;53:517–525.
20 Wieronska JM, Szewczyk B, Branski P, Palucha A, Pilc A. Antidepressant-like effect of MPEP, a potent, selective and systemically active mGlu5 receptor antagonist in the olfactory bulbectomized rats. Amino Acids. 2002;23:213–216.
21 Saitoh A, Yamada M, Yamada M, Takahashi K, Yamaguchi K, Murasawa H, et al. Antidepressant-like effects of the delta-opioid receptor agonist SNC80 ([(+)-4-[(alphaR)-alpha-[(2S,5R)-2,5-dimethyl-4-(2-propenyl)-1-piperazinyl]-(3-methoxyphenyl) methyl]-N,N-diethylbenzamide) in an olfactory bulbectomized rat model. Brain Res. 2008;1208:160–169.
22 Filliol D, Ghozland S, Chluba J, Martin M, Matthes HW, Simonin F, et al. Mice deficient for delta- and mu-opioid receptors exhibit opposing alterations of emotional responses. Nat Genet. 2000;25:195–200.
23 Tejedor-Real P, Mico JA, Smadja C, Maldonado R, Roques BP, Gilbert-Rahola J. Involvement of delta-opioid receptors in the effects induced by endogenous enkephalins on learned helplessness model. Eur J Pharmacol. 1998;354:1–7.
24 Baamonde A, Dauge V, Ruiz-Gayo M, Fulga IG, Turcaud S, Fournie-Zaluski MC, et al. Antidepressant-type effects of endogenous enkephalins protected by systemic RB 101 are mediated by opioid delta and dopamine D1 receptor stimulation. Eur J Pharmacol. 1992;216:157–166.
25 Brady JV, Nauta WJ. Subcortical mechanisms in emotional behavior: the duration of affective changes following septal and habenular lesions in the albino rat. J Comp Physiol Psychol. 1955;48:412–420.
26 Shibata S, Nakanishi H, Watanabe S, Ueki S. Effects of chronic administration of antidepressants on mouse-killing behavior (muricide) in olfactory bulbectomized rats. Pharmacol Biochem Behav. 1984;21:225–230.
27 Yamada M, Iwabuchi T, Takahashi K, Kurahashi C, Ohata H, Honda K, et al. Identification and expression of frizzled-3 protein in rat frontal cortex after antidepressant and electroconvulsive treatment. J Pharmacol Sci. 2005;99:239–246.
28 Hubbell E, Liu WM, Mei R. Robust estimators for expression analysis. Bioinformatics. 2002;18:1585–1592.
29 Dennis G Jr, Sherman BT, Hosack DA, Yang J, Gao W, Lane HC, et al. DAVID: Database for Annotation, Visualization, and Integrated Discovery. Genome Biol. 2003;4:P3.
30 Saitoh A, Yamaguchi K, Tatsumi Y, Murasawa H, Nakatani A, Hirose N, et al. Effects of milnacipran and fluvoxamine on hyperemotional behaviors and the loss of tryptophan hydroxylase-positive cells in olfactory bulbectomized rats. Psychopharmacology (Berl). 2007;191:857–865.
31 Drevets WC, Videen TO, Price JL, Preskorn SH, Carmichael ST, Raichle ME. A functional anatomical study of unipolar depression. J Neurosci. 1992;12:3628–3641.
32 Gunther EC, Stone DJ, Gerwien RW, Bento P, Heyes MP. Prediction of clinical drug efficacy by classification of drug-induced genomic expression profiles in vitro. Proc Natl Acad Sci U S A. 2003;100:9608–9613.
33 Tan PK, Downey TJ, Spitznagel EL Jr, Xu P, Fu D, Dimitrov DS, et al. Evaluation of gene expression measurements from commercial microarray platforms. Nucleic Acids Res. 2003;31: 5676–5684.
34 Yauk CL, Berndt ML, Williams A, Douglas GR. Comprehensive

comparison of six microarray technologies. Nucleic Acids Res. 2004;32:e124.
35 Bammler T, Beyer RP, Bhattacharya S, Boorman GA, Boyles A, Bradford BU, et al. Standardizing global gene expression analysis between laboratories and across platforms. Nat Methods. 2005;2:351–356.
36 Irizarry RA, Warren D, Spencer F, Kim IF, Biswal S, Frank BC, et al. Multiple-laboratory comparison of microarray platforms. Nat Methods. 2005;2:345–350.
37 Larkin JE, Frank BC, Gavras H, Sultana R, Quackenbush J. Independence and reproducibility across microarray platforms. Nat Methods. 2005;2:337–344.
38 Sherlock G. Of fish and chips. Nat Methods. 2005;2:329–330.
39 Maes M, De Vos N, Demedts P, Wauters A, Neels H. Lower serum zinc in major depression in relation to changes in serum acute phase proteins. J Affect Disord. 1999;56:189–194.
40 Maes M, Vandoolaeghe E, Neels H, Demedts P, Wauters A, Meltzer HY, et al. Lower serum zinc in major depression is a sensitive marker of treatment resistance and of the immune /inflammatory response in that illness. Biol Psychiatry. 1997;42:349–358.
41 Nowak G, Siwek M, Dudek D, Zieba A, Pilc A. Effect of zinc supplementation on antidepressant therapy in unipolar depression: a preliminary placebo-controlled study. Pol J Pharmacol. 2003;55:1143–1147.
42 Kroczka B, Branski P, Palucha A, Pilc A, Nowak G. Antidepressant-like properties of zinc in rodent forced swim test. Brain Res Bull. 2001;55:297–300.
43 Szewczyk B, Branski P, Wieronska JM, Palucha A, Pilc A, Nowak G. Interaction of zinc with antidepressants in the forced swimming test in mice. Pol J Pharmacol. 2002;54:681–685.
44 Rosa AO, Lin J, Calixto JB, Santos AR, Rodrigues AL. Involvement of NMDA receptors and L-arginine-nitric oxide pathway in the antidepressant-like effects of zinc in mice. Behav Brain Res. 2003;144:87–93.
45 Nowak G, Szewczyk B, Wieronska JM, Branski P, Palucha A, Pilc A, et al. Antidepressant-like effects of acute and chronic treatment with zinc in forced swim test and olfactory bulbectomy model in rats. Brain Res Bull. 2003;61:159–164.
46 Nowak G, Szewczyk B, Pilc A. Zinc and depression. An update. Pharmacol Rep. 2005;57:713–718.
47 Cieslik K, Klenk-Majewska B, Danilczuk Z, Wrobel A, Lupina T, Ossowska G. Influence of zinc supplementation on imipramine effect in a chronic unpredictable stress (CUS) model in rats. Pharmacol Rep. 2007;59:46–52.
48 Uhr M, Grauer MT, Holsboer F. Differential enhancement of antidepressant penetration into the brain in mice with abcb1ab (mdr1ab) P-glycoprotein gene disruption. Biol Psychiatry. 2003;54:840–846.
49 Uhr M, Steckler T, Yassouridis A, Holsboer F. Penetration of amitriptyline, but not of fluoxetine, into brain is enhanced in mice with blood-brain barrier deficiency due to mdr1a P-glycoprotein gene disruption. Neuropsychopharmacology. 2000; 22:380–387.
50 Seelig A. A general pattern for substrate recognition by P-glycoprotein. Eur J Biochem. 1998;251:252–261.
51 Hennessy M, Kelleher D, Spiers JP, Barry M, Kavanagh P, Back D, et al. St Johns wort increases expression of P-glycoprotein: implications for drug interactions. Br J Clin Pharmacol. 2002;53:75–82.
52 Uz T, Ahmed R, Akhisaroglu M, Kurtuncu M, Imbesi M, Dirim Arslan A, et al. Effect of fluoxetine and cocaine on the expression of clock genes in the mouse hippocampus and striatum. Neuroscience. 2005;134:1309–1316.
53 Uz T, Manev H. Chronic fluoxetine administration increases the serotonin N-acetyltransferase messenger RNA content in rat hippocampus. Biol Psychiatry. 1999;45:175–179.
54 Popsueva AE, Luchinskaya NN, Ludwig AV, Zinovjeva OY, Poteryaev DA, Feigelman MM, et al. Overexpression of camello, a member of a novel protein family, reduces blastomere adhesion and inhibits gastrulation in Xenopus laevis. Dev Biol. 2001;234:483–496.
55 Kim JS, Schmid-Burgk W, Claus D, Kornhuber HH. Increased serum glutamate in depressed patients. Arch Psychiatr Nervenkr. 1982;232:299–304.
56 Altamura C, Maes M, Dai J, Meltzer HY. Plasma concentrations of excitatory amino acids, serine, glycine, taurine and histidine in major depression. Eur Neuropsychopharmacol. 1995;5 Suppl: 71–75.
57 Levine J, Panchalingam K, Rapoport A, Gershon S, McClure RJ, Pettegrew JW. Increased cerebrospinal fluid glutamine levels in depressed patients. Biol Psychiatry. 2000;47:586–593.
58 Auer DP, Putz B, Kraft E, Lipinski B, Schill J, Holsboer F. Reduced glutamate in the anterior cingulate cortex in depression: an in vivo proton magnetic resonance spectroscopy study. Biol Psychiatry. 2000;47:305–313.
59 Sanacora G, Gueorguieva R, Epperson CN, Wu YT, Appel M, Rothman DL, et al. Subtype-specific alterations of gamma-aminobutyric acid and glutamate in patients with major depression. Arch Gen Psychiatry. 2004;61:705–713.
60 Ongur D, Drevets WC, Price JL. Glial reduction in the subgenual prefrontal cortex in mood disorders. Proc Natl Acad Sci U S A. 1998;95:13290–13295.
61 Rajkowska G, Miguel-Hidalgo JJ, Wei J, Dilley G, Pittman SD, Meltzer HY, et al. Morphometric evidence for neuronal and glial prefrontal cell pathology in major depression. Biol Psychiatry. 1999;45:1085–1098.
62 Cotter D, Mackay D, Landau S, Kerwin R, Everall I. Reduced glial cell density and neuronal size in the anterior cingulate cortex in major depressive disorder. Arch Gen Psychiatry. 2001;58:545–553.
63 Choudary PV, Molnar M, Evans SJ, Tomita H, Li JZ, Vawter MP, et al. Altered cortical glutamatergic and GABAergic signal transmission with glial involvement in depression. Proc Natl Acad Sci U S A. 2005;102:15653–15658.
64 Michael-Titus AT, Bains S, Jeetle J, Whelpton R. Imipramine and phenelzine decrease glutamate overflow in the prefrontal cortex – a possible mechanism of neuroprotection in major depression? Neuroscience. 2000;100:681–684.
65 Wang SJ, Su CF, Kuo YH. Fluoxetine depresses glutamate exocytosis in the rat cerebrocortical nerve terminals (synaptosomes) via inhibition of P/Q-type Ca2+ channels. Synapse. 2003;48:170–177.
66 Bonanno G, Giambelli R, Raiteri L, Tiraboschi E, Zappettini S, Musazzi L, et al. Chronic antidepressants reduce depolarization-evoked glutamate release and protein interactions favoring formation of SNARE complex in hippocampus. J Neurosci. 2005;25:3270–3279.
67 Takahashi K, Yamada M, Ohata H, Momose K, Higuchi T, Honda K. Expression of Ndrg2 in the rat frontal cortex after antidepressant and electroconvulsive treatment. Int J Neuropsychopharmacol. 2005;8:381–389.